

Calibrated Uncertainty for Molecular Property Prediction using Ensembles of Message Passing Neural Networks

Jonas Busk^{1,*} Peter Bjørn Jørgensen¹ Arghya Bhowmik¹
 Mikkel N. Schmidt² Ole Winther^{2,3,4} Tejs Vegge¹

¹Department for Energy Conversion and Storage, Technical University of Denmark, Lyngby, Denmark

²Department of Applied Mathematics and Computer Science, Technical University of Denmark, Lyngby, Denmark

³Center for Genomic Medicine, Rigshospitalet, Copenhagen University Hospital, Copenhagen, Denmark

⁴Bioinformatics Centre, Department of Biology, University of Copenhagen, Copenhagen, Denmark

*Corresponding author: Jonas Busk, jbusk@dtu.dk

Abstract

Data-driven methods based on machine learning have the potential to accelerate analysis of atomic structures. However, machine learning models can produce overconfident predictions and it is therefore crucial to detect and handle uncertainty carefully. Here, we extend a message passing neural network designed specifically for predicting properties of molecules and materials with a calibrated probabilistic predictive distribution. The method presented in this paper differs from the previous work by considering both aleatoric and epistemic uncertainty in a unified framework, and by re-calibrating the predictive distribution on unseen data. Through computer experiments, we show that our approach results in accurate models for predicting molecular formation energies with calibrated uncertainty in and out of the training data distribution on two public molecular benchmark datasets, QM9 and PC9. The proposed method provides a general framework for training and evaluating neural network ensemble models that are able to produce accurate predictions of properties of molecules with calibrated uncertainty.

1 Introduction

Autonomous high-throughput computational analysis of atomic structures has the potential to speed up the discovery of novel materials and chemical reactions

dramatically with applications in a wide range of research areas like biotechnology and conversion and storage of renewable energy. This process can be enabled and accelerated by data-driven methods based on machine learning that are less computationally demanding than traditional quantum mechanical methods such as density functional theory (DFT) [1]. In recent years, graph-based models such as message passing neural networks (MPNNs), that operate on atomic structures represented as graphs, have shown impressive capabilities at predicting properties of molecules and materials with high accuracy [2]. However, deep neural networks are known to produce overconfident predictions [3], especially outside the training data distribution, which can lead to sub-optimal or incorrect results. Because chemical space is too vast to represent in any training dataset [4, 5], in an autonomous high-throughput setting it is crucial to detect and handle predictive uncertainty, for example by falling back to more accurate but computationally demanding methods like DFT [6]. Consequently, predictive algorithms that express probabilistic uncertainty about predictions can help identify problematic instances and thereby enable the design of new robust workflows [7] and applications in computational materials research.

When quantifying uncertainty it is often useful to distinguish between *epistemic* and *aleatoric* uncertainty [8, 9]. Epistemic uncertainty arises from the model’s inability to fit the data distribution and can in principle be reduced by observing more data or improving the model. Aleatoric uncertainty on the other hand comes from inherent noise in the data and can therefore not be reduced by observing more data. When the aleatoric uncertainty is constant across all observations it is called *homoscedastic* aleatoric uncertainty and is often not modelled explicitly. If the aleatoric uncertainty depends on the input, and thus varies across the data distribution, it is called *heteroscedastic* aleatoric uncertainty and can be estimated from the data by explicitly including it in the model. Thus epistemic uncertainty is important for understanding when predictions can be trusted and aleatoric uncertainty captures noise in the data. Consequently, both types of uncertainty are necessary to obtain a complete picture of the predictive uncertainty and provide important information for interpretability and decision making.

In this work, we extend a message passing neural network regression model designed specifically for predicting properties of molecules and materials [10] with a probabilistic predictive distribution and consider a deep ensemble of models [11] to express the aleatoric and epistemic uncertainty about predictions of molecular formation energies. The predicted uncertainty is re-calibrated to fit the error distribution on unseen data to address model overconfidence from training and the expected improved accuracy from using an ensemble approximation. We show through computer experiments that our approach results in well calibrated models on two public benchmark datasets for molecular property prediction, QM9 [12] and PC9 [13]. The main contribution of this paper is a complete framework for training and evaluating neural network models that are able to produce accurate predictions of properties of molecules with calibrated aleatoric and epistemic uncertainty estimates.

Uncertainty quantification for property prediction of atomic structures with

graph neural networks has received increasing interest recently. Scalia et al. [14] evaluated and compared scalable uncertainty estimation methods based on graph neural networks for molecular property prediction and found that deep ensembles [11] and bootstrapping consistently outperformed Monte Carlo Dropout [15] on multiple public benchmark datasets in terms of error and uncertainty calibration. Tran et al. [16] highlight the importance of predictive uncertainty in materials screening applications and review methods for uncertainty quantification and procedures for evaluating the quality of uncertainty estimates including accuracy, calibration and sharpness. Nigam et al. [17] provide an extensive overview of different sources of uncertainty in molecular property prediction in the context of drug discovery, many of which are also relevant in materials research, and describe the importance and perspectives of having good uncertainty estimates in data driven decision making. Related work has studied the use of Gaussian Process Regression models for molecular property prediction [18] and molecular dynamics [19]. The method presented in this paper differs from the previous work by considering both aleatoric and epistemic uncertainty in a unified framework, and by re-calibrating the uncertainty estimates to obtain more accurate uncertainties on unseen data.

The rest of the paper is organised as follows. The proposed method is introduced in Section 2 and experiments and results are presented in Section 3. The main findings and perspectives are discussed in Section 4 and we conclude in Section 5.

2 Method

2.1 Message passing neural network model

In general, a message passing neural network (MPNN), as described in [2], operates on a graph structure g with node features x_v and edge features e_{vw} , where v and w denote vertices in the graph. A forward pass through the neural network consists of two phases: i) a message passing phase with T interaction steps where messages are passed along the edges of the graph to update the internal graph embedding, and ii) a readout phase where an output value \hat{y} is computed from the final graph embedding.

We base our work on the SchNet with edge updates MPNN model, which was previously introduced by the authors [10]. This model is in turn based on the SchNet model, that was designed specifically for predicting properties of molecules and materials [20]. We refer the reader to the cited literature for specific details about the neural network architecture. It is worth noting that the uncertainty quantification method proposed in the following sections does not depend on the particular choice of neural network base model and can thus be adapted to use other models based on the specific application.

2.2 Extended model with predictive uncertainty

To capture both epistemic and heteroscedastic aleatoric uncertainty, we extend the MPNN described in the previous section by constructing a deep ensemble of networks [11] (without adversarial training) in the following way. Given a regression task with a training dataset $\mathcal{D} = \{g_n, y_n\}_{n=1}^N$ consisting of N datapoints with real-valued targets $y \in \mathbb{R}$, we consider an ensemble of M neural network models with parameters $\{\theta_m\}_{m=1}^M$, each with probabilistic predictive distribution:

$$p_\theta(y|g) = \mathcal{N}(\mu_\theta(g), \sigma_\theta^2(g)), \quad (1)$$

assuming a normal distribution of errors. Each network is constructed with two outputs corresponding to the predicted mean $\mu_\theta(g)$ and variance $\sigma_\theta^2(g)$, where the latter represents the predicted heteroscedastic aleatoric uncertainty [21]. The predicted variance is constrained to be positive by passing the second network output through the softplus function, $\log(1 + \exp(\cdot))$, and adding a small minimum variance for numerical stability (e.g. 10^{-6}).

2.3 Model training procedure

Each network of the ensemble is initialized with random parameters and trained individually (on the same training set) using stochastic gradient descent to minimise the negative log likelihood (NLL) loss:

$$\text{NLL}(\theta) = \frac{1}{N} \sum_{n=1}^N -\log p_\theta(y_n|g_n) \quad (2)$$

$$= \frac{1}{N} \sum_{n=1}^N \frac{1}{2} \left(\underbrace{\frac{1}{\sigma_\theta^2(g_n)} (y_n - \mu_\theta(g_n))^2}_{\text{squared error}} + \log \sigma_\theta^2(g_n) + \underbrace{\log 2\pi}_{\text{constant}} \right). \quad (3)$$

The last term in (3) is constant since it does not depend on $\mu_\theta(g)$ or $\sigma_\theta^2(g)$ and can be ignored for the purpose of training the model. Notice how for constant variance (homoscedastic uncertainty) this is equivalent to minimising the standard mean squared error (MSE) loss. Notice also how the predicted uncertainty acts as learned loss attenuation by letting examples with high predicted uncertainty have smaller impact on the total loss, while the $\log \sigma_\theta^2$ term discourages large uncertainties [9].

In practice, we found that training directly with NLL loss can be unstable because of interactions between the mean and variance output in the loss function. To mitigate this, we initially train the mean output of the network before introducing the variance terms by interpolating from MSE to NLL loss:

$$\mathcal{L}(\theta) = \lambda \text{MSE}(\theta) + (1 - \lambda) \text{NLL}(\theta), \quad (4)$$

where λ is set to 1 for a number of warmup steps and then decreased linearly from 1 to 0 over a number of interpolation steps. The resulting loss function is quite natural since the NLL loss includes the squared error term (see eq. 3) and

as a result we found that model training becomes more stable and robust to outliers in the training data. Additional measures exist to promote the stability of training variance networks [21, 22, 23], but we found the method above to be sufficient in this case.

2.4 Ensemble mixture

To produce the ensemble predictive distribution $p_*(y|g)$ and capture epistemic uncertainty, we follow the approach of [11] and make an ensemble approximation by combining the predictions of the M individual models as a uniformly-weighted mixture of normal distributions:

$$p_*(y|g) = \frac{1}{M} \sum_{m=1}^M p_{\theta_m}(y|g), \quad (5)$$

whose mean $\mu_*(g)$ and variance $\sigma_*^2(g)$ are given by the following expressions:

$$\mu_*(g) = \frac{1}{M} \sum_{m=1}^M \mu_{\theta_m}(g), \quad (6)$$

$$\sigma_*^2(g) = \frac{1}{M} \sum_{m=1}^M (\sigma_{\theta_m}^2(g) + \mu_{\theta_m}^2(g)) - \mu_*^2(g) \quad (7)$$

$$= \underbrace{\frac{1}{M} \sum_{m=1}^M \sigma_{\theta_m}^2(g)}_{\text{aleatoric uncertainty}} + \underbrace{\frac{1}{M} \sum_m \mu_{\theta_m}^2(g) - \mu_*^2(g)}_{\text{epistemic uncertainty}}. \quad (8)$$

The variance of the ensemble predictive distribution represents the total predicted uncertainty and can be decomposed into aleatoric and epistemic uncertainty as shown in eq. 8 above.

2.5 Uncertainty calibration

Training with NLL loss can result in overfitting of the uncertainty to the training data once a good fit for the mean is found [21]. This can lead to overconfident predictions as we expect the model to have higher error, and thus higher uncertainty, when presented with unseen data. On the other hand, using an ensemble of models can reduce the overall error, and should thus lead to lower uncertainty. This is not reflected in the ensemble variance (eq. 8) which is strictly higher than the average of the individual variances. Furthermore, there is nothing in the training procedure which ensures that the epistemic uncertainty fits the error distribution. Thus there is a need to re-calibrate the uncertainty to unseen data. This can be achieved by applying a calibration function, that maps the predictive distribution to a calibrated distribution.

Several approaches to re-calibrate regression models have been proposed in the literature [24, 25, 26]. A simple, yet robust, method is to simply scale the

predicted uncertainty estimates by a scaling factor s_n^2 optimised to fit the error distribution on unseen data [25]. Uncertainty scaling has the advantage that it does not modify the mean prediction and the calibrated predictive distribution remains a normal distribution:

$$p_{s^2}(y_n|g_n) = \mathcal{N}(\mu_*(g_n), s_n^2 \sigma_*^2(g_n)). \quad (9)$$

The solution proposed in [25] is to scale all uncertainty estimates by a constant scaling factor optimised to minimise the NLL on a held out calibration dataset, but it was also suggested to use non-linear methods. We found that with our method better calibration results were achieved by applying a non-linear function to scale the uncertainty estimates. Specifically, to obtain the scaled uncertainty estimates we apply an isotonic regression model¹ $f_\phi(\cdot)$ to fit the empirical squared errors $(y_n - \mu_\theta(g_n))^2$ on a held out calibration dataset:

$$s_n^2 \sigma_*^2(g_n) = f_\phi(\sigma_*^2(g_n)). \quad (10)$$

The isotonic regression results in a monotonic increasing scaling function and thus has the desired property of being non-linear while maintaining the overall ordering of the uncertainty estimates.

2.6 Evaluating the uncertainty calibration

Evaluating uncertainty estimates in regression tasks is not straight forward as the true uncertainties are generally unknown [24, 25, 26]. In the classification domain, a classifier is said to be calibrated, if the predicted class probability corresponds to the probability that the prediction is correct. In other words, the classifier is expected to correctly predict its error. In a similar way, calibration for regression can be defined as correctly predicting the expected error for each data point [25].

The NLL is the standard metric for evaluating the quality of probabilistic models by measuring the probability of observing the data given the predicted distribution. In regression, the NLL depends both on the predicted mean and variance, but it is also useful to evaluate the predicted uncertainty on its own. To evaluate the uncertainty calibration of a model, we can thus compare the predicted uncertainties to the observed errors on a test dataset. To do this, we sort examples by their predicted uncertainty, divide them into K bins and in each bin k compute the predicted root mean variance (RMV) and the empirical root mean squared error (RMSE). The resulting values can be used to produce a reliability diagram where RMSE is plotted as a function of RMV [25]. For a well calibrated model, the plotted points should lie close to the diagonal line corresponding to the identity function. The calibration error can then be summarized by the expected normalized calibration error (ENCE):

$$\text{ENCE} = \frac{1}{K} \sum_{k=1}^K \frac{|\text{RMV}_k - \text{RMSE}_k|}{\text{RMV}_k}. \quad (11)$$

¹Specifically, we use the implementation of isotonic regression available from the scikit-learn Python package [27]: `sklearn.isotonic.IsotonicRegression`.

This quantity is analogous to the expected calibration error (ECE) often used in classification [25].

Additionally, it is useful to assess the dispersion of the uncertainty estimates by computing the coefficient of variation (CV) [25]:

$$\text{CV} = \frac{\sqrt{\frac{1}{N} \sum_{n=1}^N (\sigma_*(g_n) - \mu_{\sigma_*})^2}}{\mu_{\sigma_*}}, \quad (12)$$

where $\sigma_*(g_n)$ is the predicted standard deviation (uncertainty) of instance n , $\mu_{\sigma_*} = \frac{1}{N} \sum_{n=1}^N \sigma_*(g_n)$ is the mean predicted standard deviation and N in this case iterates over the test dataset. A high CV indicates large dispersion (heteroscedasticity) of the uncertainty estimates and thus a high input dependence, whereas a CV of zero indicates constant (homoscedastic) uncertainty and consequently the uncertainty estimates are uninformative.

As a secondary diagnostic tool we can compare the predicted quantiles to the observed quantiles averaged over the entire test dataset [24]. Visualising these quantities in a calibration plot reveals if the predictive distribution fits the error distribution on average. For a well calibrated model, the plotted line should lie close to the diagonal. The quantile calibration can be summarised by the sum of squared errors (SE) between the predicted and observed quantiles.

3 Experiments and results

3.1 Datasets

In our experiments we consider two publicly available datasets: QM9 [12], which is a widely used benchmark for machine learning predictions of molecular properties, and the more recent PC9 [13], that contains a more diverse set of molecules, but with the same general constraints as QM9.

The QM9 dataset consists of 133,885 small organic molecules in equilibrium state with up to 9 heavy atoms (C, O, N, F) besides hydrogen. For each molecule, the dataset contains several quantum chemical properties calculated at the B3LYP/6-31G(2df,p) level of theory including total energy U_0 , which incorporates the vibrational zero point energy (ZPE) [12]. We additionally compute the total energy without the ZPE, $E = U_0 - \text{ZPE}$, to enable comparison with PC9, that does not include U_0 . The PC9 dataset [13] consists of 99,234 molecules extracted from the PubChem database [28] by applying the constraints of QM9 mentioned above and was found to represent a more diverse set of molecules than QM9. PC9 includes properties calculated at the B3LYP/6-31G(d) level of theory including total energy E . Structures that appear in both datasets were identified by comparing International Chemical Identifiers (InChI) [29] (see supplementary material A for details). We found that 21,777 molecules from QM9 are also in PC9 and 21,619 molecules from PC9 are also in QM9.

In line with previous work, we actually consider the atomisation energies (the energy remaining after subtracting the energies of the constituent atoms)

Dataset			Error (eV)		Calibration		
Train	Test	Target	MAE	RMSE	NLL	ENCE	CV
QM9	QM9	U_0	0.0094	0.0313	-3.1593	0.0484	1.8939
QM9	QM9	E	0.0101	0.0342	-3.0759	0.0720	1.7293
PC9	PC9	E	0.0199	0.0844	-2.5956	0.0650	2.2011
QM9	PC9	E	0.4192	0.7410	0.8107	0.0220	0.6294
PC9	QM9	E	0.1165	0.1737	-0.5366	0.0312	0.5597

Table 1: Test results of ensemble models trained to predict atomisation energy properties on the QM9 and PC9 datasets. Mean absolute error (MAE) and root mean squared error (RMSE) are presented in electron volt (eV). The uncertainty calibration in each experiment is summarised by the mean negative log likelihood (NLL), expected normalised calibration error (ENCE), and coefficient of variation (CV) of the uncertainty estimates.

in our experiments, rather than the total energies. Thus in subsequent sections, U_0 and E will be used to refer to the respective atomisation energies.

3.2 Experimental setup

To evaluate the proposed method, we performed experiments of predicting atomisation energies on the QM9 and PC9 datasets. In each experiment, we trained a deep ensemble of $M = 5$ message passing neural network models extended to predict uncertainty as described in Section 2. The models were trained individually using the same hyperparameters and data splits, but with random parameter initialisation and random shuffling of the training data to induce model diversity. Following previous work [10], the networks were constructed with $T = 3$ interaction steps, a cutoff distance of 5.0 Å for constructing the molecular graphs, and an embedding size of 256 nodes in each layer. We used the PyTorch implementation of the AdamW optimizer [30] with an initial learning rate of 0.0001, an exponential decay learning rate scheduler, and a weight decay coefficient of 0.01. Each model was trained for up to 3,000,000 gradient steps with 1,000,000 warmup steps training only with MSE loss ($\lambda = 1$) and loss interpolated linearly from MSE to NLL on the subsequent 1,000,000 steps (see eq. 4). The validation set was used for early stopping with NLL criterion and was also used as calibration set for fitting the calibration function f_ϕ as described in Section 2.5.

3.3 Prediction of U_0 on QM9 with random split

In this first experiment, we trained an ensemble to predict the total energy U_0 property of the QM9 dataset. Following previous work [2, 10, 20], we randomly split the data into a training set of 110,000 molecules, a validation set of 10,000 molecules, and a test set consisting of the remaining 13,885 molecules. The test

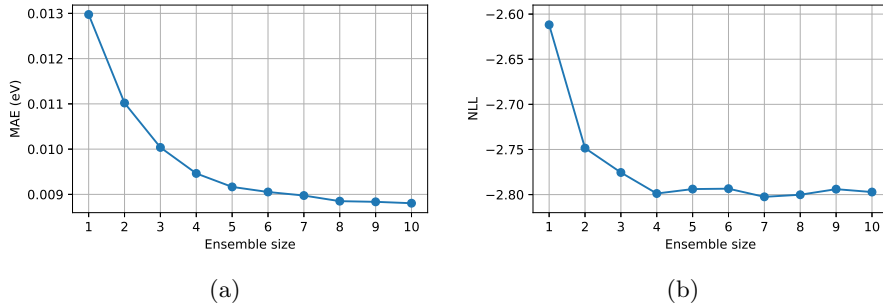


Figure 1: Trade off between error and ensemble size evaluated on the QM9 validation set when predicting the U_0 property: (a) mean absolute error (MAE) in eV and (b) mean negative log likelihood (NLL). The models are sorted by NLL in increasing order (best first). Reasonably low errors can be achieved with an ensemble size of $M = 5$ models.

set results are presented in the first row of Table 1. The ensemble achieved a MAE = 0.0094 eV which is comparable to previous work using a similar model [10] (MAE = 0.0105 eV).

Figure 1 shows the trade off between error and ensemble size of up to 10 models on the validation set. As expected, using a larger ensemble clearly improves the error. In this case, reasonably low errors can be achieved with an ensemble of $M = 5$ models and not much is gained by increasing the size of the ensemble beyond that, so we choose to use ensembles of this size throughout our experiments. Similar behavior was observed for all experiments.

The ensemble uncertainty estimates were re-calibrated by fitting an isotonic regression calibration function (see Section 2.5) on the validation set and applying it on the test set leading to an average scaling factor of 0.2965 (SD = 0.5346) on the test set. Even though each individual model is expected to have increased error when presented with unseen data, the ensemble approximation significantly improved the overall error in this case resulting in a calibration function that effectively shrinks the uncertainty of the predictive distribution. Uncertainty calibration diagrams are presented in Figure 2 and uncertainty evaluation metrics are summarised in the first row of Table 1. The reliability diagram shows that in general the model assigns higher uncertainty to instances with higher error and overall the model is well calibrated since the predicted uncertainties correspond closely to the observed errors on average, placing the points close to the diagonal. The rightmost bin, representing predictions with the highest uncertainty estimates, includes instances with relatively large errors, placing this point far from the rest. However, the model correctly assigns high uncertainty to these instances, thereby identifying them as problematic. The diagram also reveals that epistemic uncertainty is relatively low in most cases, indicating a high level of agreement among the individual models of the ensemble, and consequently the aleatoric uncertainty is responsible for the majority of

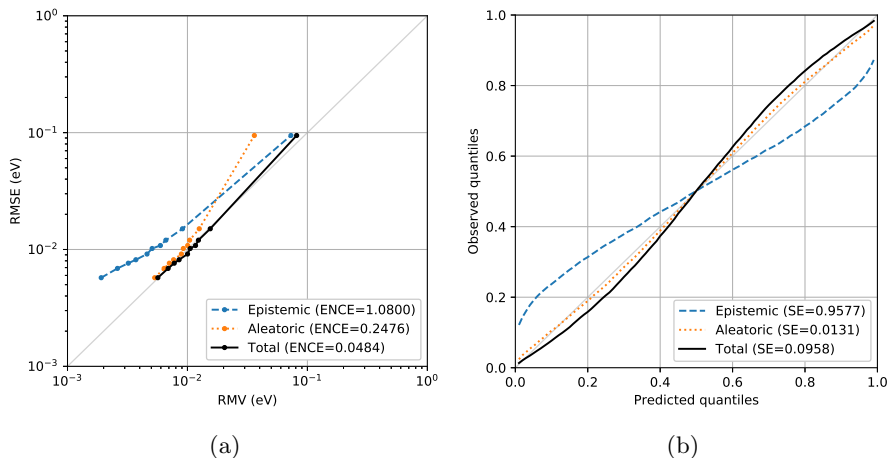


Figure 2: Evaluation of uncertainty on the QM9 test set when predicting the U_0 property. The reliability diagram (a) shows observed root mean squared error (RMSE) as a function of predicted uncertainty measured by root mean variance (RMV) computed in bins. The error is measured by expected normalized calibration error (ENCE). The calibration plot (b) compares predicted quantiles and observed quantiles averaged over the test data. The error is measured by the sum of squared errors (SE).

the total uncertainty in these cases. The last bin is an exception showing high epistemic uncertainty, corresponding to a high level of disagreement among the individual models, indicating these molecules are out of distribution and therefore the predictions are also more likely to have high error. Additionally, the uncertainty estimates have a CV (eq. 12) well above 0, indicating that the uncertainties assigned by the model have large dispersion and thus are highly input dependent.

Learning curves for this experiment are presented in Figure 3 showing test set metrics as a function of the amount of training data when predicting U_0 on QM9. As expected, the error metrics decrease with more training data. Interestingly, good calibration in terms of the ENCE was obtained with relatively small training datasets and does not vary significantly when adding more data, while the dispersion of uncertainty estimates measured by the CV clearly increases with the amount of training data, making the uncertainty estimates more input dependent and thus more informative.

3.4 Prediction of E on QM9 with random split

Complementary to the first experiment, we also trained an ensemble to predict the total energy E of the QM9 dataset using the same data split. The test set results are presented in the second row of Table 1. The ensemble model achieved a MAE = 0.0101 eV, which is a little higher than when predicting U_0 ,

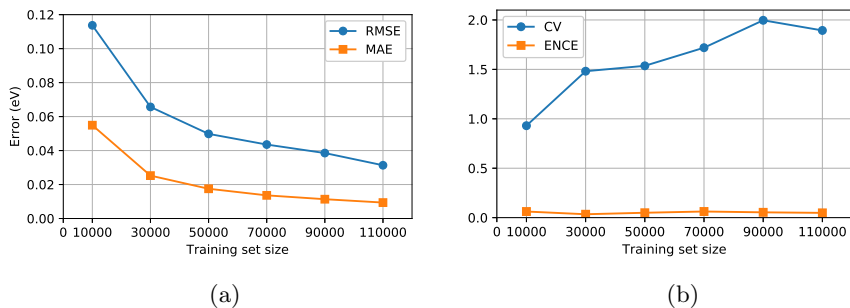


Figure 3: Learning curves showing test set metrics as a function of training set size on the QM9 dataset when predicting U_0 . (a) The mean absolute error (MAE) and root mean squared error (RMSE) improve with more data as expected. (b) The calibration in terms of expected normalised calibration error (ENCE) does not vary significantly, while the dispersion of uncertainty estimates measured by the coefficient of variation (CV) increases with the amount of training data.

suggesting predicting E is harder. A similar finding was reported in [13] using a SchNet [20] model.

The uncertainty estimates were likewise re-calibrated by fitting an isotonic regression calibration function on the validation set and applying it on the test set leading to an average scaling factor of 0.3116 (SD = 0.3966) on the test set, effectively shrinking the predictive distribution similarly to the first experiment. Also in this case we found that the model succeeds at assigning uncertainty estimates that correlates with the error and the model is well calibrated. Both ENCE and CV results are similar to the first experiment. Uncertainty calibration figures for this experiment are included in the supplementary material B1.

3.5 Prediction of E on PC9 with random split

Next, we trained an ensemble to predict the total energy E of the more diverse PC9 dataset. The data was split randomly into a training set of 80,000 molecules, a validation set of 10,000 molecules, and a test set consisting of the remaining 9,234 molecules. The test set results are presented in the third row of Table 1. The ensemble model achieved a MAE = 0.0199 eV which is approximately twice as high as when predicting E on QM9. We attribute this increase in error to PC9 representing a more diverse set of molecules, making the task more difficult, and additionally to the smaller amount of available training data. A similar increase in error between QM9 and PC9 was reported in [13] using a SchNet [20] model.

The uncertainty estimates were re-calibrated by fitting a calibration function on the validation set and applying it on the test set leading to an average scaling factor of 0.2938 (SD = 0.6449) on the test set, effectively shrinking the uncer-

tainty of the predictive distribution similarly to the two previous experiments. This model also succeeds in assigning uncertainty estimates that correlates with the observed error and the model is well calibrated. As in the two previous experiments, some instances among the predictions with the highest uncertainty have relatively large errors. The ENCE is similar to the two previous experiments while the CV is higher, indicating more dispersion of the uncertainty estimates corresponding to the overall increase in error. Uncertainty calibration figures for this experiment are included in the supplementary material B2.

3.6 Generalisation from QM9 to PC9

In this experiment we examine the effect of applying an ensemble of models trained on QM9 to the more diverse set of molecules included in PC9 and especially how it affects the uncertainty estimates as we anticipate larger errors. When constructing the data splits, we utilize the fact that the datasets are overlapping, using the 112,108 molecules that are unique to QM9 as the training set and the 21,777 structures from QM9 that are also present in PC9 as the validation set. Then we compute a linear correction on the 21,619 structures from PC9 that are present in QM9 to account for the different level of theory used to calculate the energy properties. Following [13], the linear correction was performed by fitting a Huber regression model (coefficient = 1.0038, intercept = 1.1428) on the predicted and observed energies. Finally, we use the remaining 77,615 molecules exclusive to PC9 as the test set and apply the linear correction to the predictions. The test set results are presented in the fourth row of Table 1. The ensemble model achieved a MAE = 0.4192 eV, which is comparable to the findings reported in [13] using a SchNet [20] model. The relatively high error is caused primarily by out of distribution instances, and indicates that the model has problems generalising under domain shift, and secondly by the different level of theory used to calculate the energies in the different datasets, which was shown to produce large errors (see Figure 3 in [13]).

The uncertainty estimates were re-calibrated by fitting an isotonic regression calibration function on the validation set and applying it on the test set leading to an average scaling factor of 135.0313 (SD = 31.5991) on the test set, reflecting the large increase in error when extrapolating to a more diverse dataset containing out of distribution molecules. Interestingly, the uncertainty estimates are still well calibrated as shown by a low ENCE, while the dispersion of the uncertainty estimates is low indicated by the relatively low CV. Uncertainty calibration figures for this experiment are included in the supplementary material B3. The calibration plot in Figure B3 shows that the predicted quantiles do not fit the observed quantiles averaged over the dataset in this experiment. This is primarily because the errors are not normally distributed in this particular case [13].

3.7 Generalisation from PC9 to QM9

Now going in the opposite direction, in this last experiment we examine the effect of applying an ensemble of models trained on PC9 to the less diverse set of molecules in QM9. Analogous to the previous experiment, we use the 77,615 molecules that are unique to PC9 as the training set and the 21,619 structures from PC9 that are also present in QM9 as the validation set. Similarly to the previous experiment, we compute a linear correction on the 21,777 structures from QM9 that are also present in PC9 by fitting a Huber regression model (coefficient = 0.9994, intercept = -0.6830) on the predicted and observed energies. Finally, we use the remaining 112,108 molecules exclusive to QM9 as the test set. The test set results are presented in the fifth and final row of Table 1. The ensemble achieved a MAE = 0.1165 eV, which is comparable to the findings in [13] using a SchNet [20] model. While high compared to the experiment of predicting E on QM9 above, the error is significantly lower than the previous experiment of training on QM9 and testing on PC9 as might be expected when going from a more diverse dataset to an overlapping and less diverse dataset. Some of the error may be attributed to the different level of theory used to calculate the energies in the datasets.

The uncertainty estimates were re-calibrated by fitting a calibration function on the validation set and applying it on the test set leading to an average scaling factor of 6.2404 (SD = 1.4109) on the test set, which like the error is also significantly lower than the previous experiment. Similarly to the previous experiment, the uncertainty remains well calibrated shown by low ENCE and the dispersion of uncertainty estimates is also relatively low in this case. Uncertainty calibration figures for this experiment are included in the supplementary material B4.

4 Discussion

In our first three experiments, we trained ensembles to predict atomisation energies on the QM9 and PC9 benchmark datasets, respectively, with random data splits. The results of predicting total energy U_0 on QM9 are comparable to previous work by the authors using the same base model [10], meaning we did not lose accuracy with our approach. We saw a small increase in the error when predicting E on QM9 which is consistent with results reported in [13]. The error when predicting E on the more diverse PC9 dataset was almost twice as high compared to QM9, which is also consistent with results reported in [13], indicating that the increase in chemical diversity makes the predictions task harder. In all three random split experiments, the proposed method produced well calibrated uncertainty estimates characterised by highly correlated average uncertainties and errors, as shown in the reliability diagram in Figure 2 and additionally in the supplementary material B, and summarized by low ENCE values (see Table 1). The reliability diagrams further show that for the test examples with high error the epistemic uncertainty is high relative to the aleatoric uncer-

tainty, indicating high variance among the predictions of the individual models in the ensemble. This means that the ensemble model is good at identifying instances that are out of distribution and therefore have high expected error, and exemplifies why it is useful to be able to distinguish between epistemic and aleatoric uncertainty in the predictions. The dispersion of uncertainty estimates, measured by the CV, was high in all three random split experiments, indicating the predicted uncertainty estimates are highly input dependent and thereby informative.

In the fourth experiment, we aimed to generalise from QM9 to the more diverse PC9 dataset by training on QM9 and testing on molecules exclusive to PC9. The analysis of the PC9 structures presented in [13] showed that some molecules included in PC9 are chemically different from molecules in QM9, making this a difficult out-of-distribution prediction task. Additionally, the properties of the datasets were computed at different levels of theory (B3LYP/6-31G(2df,p) in QM9 and B3LYP/6-31G(d) in PC9), which we accounted for with a linear correction, following [13]. The error we observed in this experiment was quite high, but comparable to what is reported in [13]. However, the uncertainty estimates of our model were still well calibrated, meaning the model is capable of correctly identifying the high error instances and assigning them high uncertainty, which means the out of distribution cases can be detected. In the fifth and final experiment, we went in the opposite direction and trained on PC9 to predict the molecules exclusively in QM9. This should be an easier task, since QM9 is similar to but less diverse than PC9. As expected, the error we observed is significantly lower than in the previous experiment and comparable to what was reported in [13]. Our method again produced calibrated uncertainty estimates, thus on average estimating the expected error of the predictions. Interestingly, the two generalisation experiments resulted in the lowest ENCE of all our experiments (see Table 1) despite having the highest errors. Additionally, in the learning curve experiment presented in Figure 3 we also observed that good calibration was achieved even for small training set sizes where the error is relatively high. As such there does not appear to be a direct correlation between error and calibration. We find this to be an interesting topic for further research.

In the proposed method, the effectiveness of the ensemble approximation, including the quality of the epistemic uncertainty estimates, relies on training a diverse set of models to ensure variance of predictions beyond the training data distribution. The method proposed in this work depends on random initialisation of network parameters and random shuffling of the training data to induce model diversity, but other more deliberate methods exist. Bootstrapping, i.e. re-sampling the training set with replacement, is a popular technique for inducing diversity in ensemble models, but some evidence suggests that this method is less appropriate for deep models as they typically perform better with more training data [11]. We tried to apply bootstrapping in our experiments, but did not observe any improvements in terms of error or calibration, so we left it out for simplicity. Another more recent approach to induce diversity is to use randomized prior functions [31], which we consider an interesting direction for

future work.

A major advantage of the proposed method is the possibility to distinguish between epistemic and aleatoric uncertainty in the predictions. Capturing epistemic uncertainty may be especially important in the area of atomic structure analysis. In some other areas, where a lot of data is available, it may be sufficient to model aleatoric uncertainty, which cannot be reduced with more data, and reduce epistemic uncertainty with large amounts of training data. Chemical space, however, is so vast that it is not feasible to gather enough training data to cover the entire domain [4, 5]. Thus, identifying cases beyond the training data distribution where the model is not expected to perform well is more critical. In particular, distinguishing between epistemic and aleatoric uncertainty can be utilised in a screening system for atomic structures in the following way: If the epistemic uncertainty of a prediction is low, the aleatoric uncertainty indicates the expected error. If, on the other hand, the epistemic uncertainty is high, there is a high level of disagreement in the ensemble and therefore low confidence in the prediction, and the system can automatically fall back to a more accurate method such as DFT [32]. The specific thresholds for decision making can be tuned depending on the data, application and computational resources available.

5 Conclusion

In this work we have explored a complete framework for obtaining well calibrated uncertainty estimates for molecular property prediction by using a deep ensemble of message passing neural networks and by re-calibrating the uncertainty estimates to unseen data. Our experiments on two publicly available benchmark datasets show that the method is able to produce well calibrated uncertainty estimates in and out of the training data distribution. A major advantage of this approach is that the uncertainty estimates can be decomposed into epistemic and aleatoric uncertainty, which allows for better interpretability and provides useful information for decision making. Additionally, the proposed method does not depend on the particular architecture of the neural network model, and can thus easily be adapted to use new models based on the specific application and as research in model development continues to advance.

6 Acknowledgements

The authors acknowledge support from the Novo Nordisk Foundation (SURE, NNF19OC0057822) and the European Union’s Horizon 2020 research and innovation program under grant agreement No 957189 (BIG-MAP) and No 957213 (BATTERY2030PLUS).

References

- [1] Pavlo O Dral. Quantum chemistry in the age of machine learning. *J. Phys. Chem. Lett.*, 11(6):2336–2347, March 2020.
- [2] Justin Gilmer, Samuel S. Schoenholz, Patrick F. Riley, Oriol Vinyals, and George E. Dahl. Neural message passing for quantum chemistry. In *Proceedings of the 34th International Conference on Machine Learning*, volume 70 of *Proceedings of Machine Learning Research*, pages 1263–1272. PMLR, 2017.
- [3] Chuan Guo, Geoff Pleiss, Yu Sun, and Kilian Q. Weinberger. On calibration of modern neural networks. In *Proceedings of the 34th International Conference on Machine Learning - Volume 70*, ICML’17, page 1321–1330. JMLR.org, 2017.
- [4] Rafael Gómez-Bombarelli, Jennifer N. Wei, David Duvenaud, José Miguel Hernández-Lobato, Benjamín Sánchez-Lengeling, Dennis Sheberla, Jorge Aguilera-Iparraguirre, Timothy D. Hirzel, Ryan P. Adams, and Alán Aspuru-Guzik. Automatic chemical design using a data-driven continuous representation of molecules. *ACS Central Science*, 4(2):268–276, 2018. PMID: 29532027.
- [5] Pavel G Polishchuk, Timur I Madzhidov, and Alexandre Varnek. Estimation of the size of drug-like chemical space based on gdb-17 data. *Journal of computer-aided molecular design*, 27(8):675–679, 2013.
- [6] Rocco Peter Fornari, Murat Mesta, Johan Hjelm, Tejs Vegge, and Piotr de Silva. Molecular engineering strategies for symmetric aqueous organic redox flow batteries. *ACS Materials Letters*, 2(3):239–246, 2020.
- [7] Felix T. Bölle, Nicolai R. Mathiesen, Alexander J. Nielsen, Tejs Vegge, Juan Maria Garcia-Lastra, and Ivano E. Castelli. Autonomous discovery of materials for intercalation electrodes. *Batteries & Supercaps*, 3(6):488–498, 2020.
- [8] Eyke Hüllermeier and Willem Waegeman. Aleatoric and epistemic uncertainty in machine learning: an introduction to concepts and methods. *Machine Learning*, 110(3):457–506, Mar 2021.
- [9] Alex Kendall and Yarin Gal. What uncertainties do we need in bayesian deep learning for computer vision? In *Proceedings of the 31st International Conference on Neural Information Processing Systems*, NIPS’17, page 5580–5590, Red Hook, NY, USA, 2017. Curran Associates Inc.
- [10] Peter Bjørn Jørgensen, Karsten Wedel Jacobsen, and Mikkel Nørgaard Schmidt. Neural message passing with edge updates for predicting properties of molecules and materials. In *Machine Learning for Molecules and Materials, Neural Information Processing Systems workshop*, 2018.

- [11] Balaji Lakshminarayanan, Alexander Pritzel, and Charles Blundell. Simple and scalable predictive uncertainty estimation using deep ensembles. *Advances in neural information processing systems*, 30:6402–6413, 2017.
- [12] Raghunathan Ramakrishnan, Pavlo O Dral, Matthias Rupp, and O Anatole Von Lilienfeld. Quantum chemistry structures and properties of 134 kilo molecules. *Scientific data*, 1(1):1–7, 2014.
- [13] Marta Glavatskikh, Jules Leguy, Gilles Hunault, Thomas Cauchy, and Benoit Da Mota. Dataset’s chemical diversity limits the generalizability of machine learning predictions. *Journal of Cheminformatics*, 11, 11 2019.
- [14] Gabriele Scalia, Colin A. Grambow, Barbara Pernici, Yi-Pei Li, and William H. Green. Evaluating scalable uncertainty estimation methods for deep learning-based molecular property prediction. *Journal of Chemical Information and Modeling*, 60(6):2697–2717, 2020. PMID: 32243154.
- [15] Yarin Gal and Zoubin Ghahramani. Dropout as a bayesian approximation: Representing model uncertainty in deep learning. In Maria Florina Balcan and Kilian Q. Weinberger, editors, *Proceedings of The 33rd International Conference on Machine Learning*, volume 48 of *Proceedings of Machine Learning Research*, pages 1050–1059, New York, New York, USA, 20–22 Jun 2016. PMLR.
- [16] Kevin Tran, Willie Neiswanger, Junwoong Yoon, Qingyang Zhang, Eric Xing, and Zachary W Ulissi. Methods for comparing uncertainty quantifications for material property predictions. *Mach. Learn.: Sci. Technol.*, 1(2):025006, May 2020.
- [17] AkshatKumar Nigam, Robert Pollice, Matthew F. D. Hurley, Riley J. Hickman, Matteo Aldeghi, Naruki Yoshikawa, Seyone Chithrananda, Vincent A. Voelz, and Alán Aspuru-Guzik. Assigning confidence to molecular property prediction. *CoRR*, abs/2102.11439, 2021.
- [18] Félix Musil, Michael J Willatt, Mikhail A Langovoy, and Michele Ceriotti. Fast and accurate uncertainty estimation in chemical machine learning. *J. Chem. Theory Comput.*, 15(2):906–915, February 2019.
- [19] Giulio Imbalzano, Yongbin Zhuang, Venkat Kapil, Kevin Rossi, Edgar A Engel, Federico Grasselli, and Michele Ceriotti. Uncertainty estimation for molecular dynamics and sampling. *J. Chem. Phys.*, 154(7):074102, February 2021.
- [20] Kristof Schütt, Pieter-Jan Kindermans, Huziel Enoc Saucedo Felix, Stefan Chmiela, Alexandre Tkatchenko, and Klaus-Robert Müller. Schnet: A continuous-filter convolutional neural network for modeling quantum interactions. *Advances in neural information processing systems*, 30:991–1001, 2017.

- [21] D. A. Nix and A. S. Weigend. Estimating the mean and variance of the target probability distribution. In *Proceedings of 1994 IEEE International Conference on Neural Networks (ICNN'94)*, volume 1, pages 55–60 vol.1, 1994.
- [22] Alexander Amini, Wilko Schwarting, Ava Soleimany, and Daniela Rus. Deep evidential regression. In H. Larochelle, M. Ranzato, R. Hadsell, M. F. Balcan, and H. Lin, editors, *Advances in Neural Information Processing Systems*, volume 33, pages 14927–14937. Curran Associates, Inc., 2020.
- [23] Nicki Skafted Detlefsen, Martin Jørgensen, and Søren Hauberg. Reliable training and estimation of variance networks. In *Proceedings of 33rd Conference on Neural Information Processing Systems*, 2019. 33rd Conference on Neural Information Processing Systems, NeurIPS 2019 ; Conference date: 08-12-2019 Through 14-12-2019.
- [24] Volodymyr Kuleshov, Nathan Fenner, and Stefano Ermon. Accurate uncertainties for deep learning using calibrated regression. In Jennifer Dy and Andreas Krause, editors, *Proceedings of the 35th International Conference on Machine Learning*, volume 80 of *Proceedings of Machine Learning Research*, pages 2796–2804. PMLR, 10–15 Jul 2018.
- [25] Dan Levi, Liran Gispán, Niv Giladi, and Ethan Fetaya. Evaluating and calibrating uncertainty prediction in regression tasks. *arXiv*, 2020.
- [26] Hao Song, Tom Diethe, Meelis Kull, and Peter Flach. Distribution calibration for regression. In Kamalika Chaudhuri and Ruslan Salakhutdinov, editors, *Proceedings of the 36th International Conference on Machine Learning*, volume 97 of *Proceedings of Machine Learning Research*, pages 5897–5906. PMLR, 09–15 Jun 2019.
- [27] F. Pedregosa, G. Varoquaux, A. Gramfort, V. Michel, B. Thirion, O. Grisel, M. Blondel, P. Prettenhofer, R. Weiss, V. Dubourg, J. Vanderplas, A. Passos, D. Cournapeau, M. Brucher, M. Perrot, and E. Duchesnay. Scikit-learn: Machine learning in Python. *Journal of Machine Learning Research*, 12:2825–2830, 2011.
- [28] Sunghwan Kim, Jie Chen, Tiejun Cheng, Asta Gindulyte, Jia He, Siqian He, Qingliang Li, Benjamin Shoemaker, Paul Thiessen, Bo Yu, Leonid Zaslavsky, Jian Zhang, and Evan Bolton. Pubchem in 2021: New data content and improved web interfaces. *Nucleic Acids Research*, 49, 11 2020.
- [29] Alan McNaught. The iupac international chemical identifier. *Chemistry international*, pages 12–14, 2006.
- [30] Ilya Loshchilov and Frank Hutter. Decoupled weight decay regularization, 2019.

- [31] Ian Osband, John Aslanides, and Albin Cassirer. Randomized prior functions for deep reinforcement learning. In S. Bengio, H. Wallach, H. Larochelle, K. Grauman, N. Cesa-Bianchi, and R. Garnett, editors, *Advances in Neural Information Processing Systems*, volume 31, pages 8617–8629. Curran Associates, Inc., 2018.
- [32] Arghya Bhowmik, Ivano E. Castelli, Juan Maria Garcia-Lastra, Peter Bjørn Jørgensen, Ole Winther, and Tejs Vegge. A perspective on inverse design of battery interphases using multi-scale modelling, experiments and generative deep learning. *Energy Storage Materials*, 21:446–456, 2019.

Supplementary material:

Calibrated Uncertainty for Molecular Property Prediction using Ensembles of Message Passing Neural Networks

A InChi comparison details

The overlapping set of structures that appear in both the QM9 [12] and PC9 [13] datasets were identified by comparing International Chemical Identifiers (InChI) strings [29]. The InChI strings for both datasets were computed using the Open Babel command line tool (obabel v. 3.1.0):

```
$ obabel [input_file.xyz] -o inchi -xr -O [output_file.inchi]
```

or similarly for multiple files:

```
$ for f in *.xyz;  
> do obabel $f -o inchi -xr -O ../inchi/${f:0:-3}inchi;  
> done
```

Then the InChi strings were truncated as to not differentiate between stereoisomers (structures with the same chemical formula and connectivity). Specifically, the /b, /t, /m, and /s layers of the InChi strings were removed. When comparing the truncated InChi strings of the two datasets, we found that that 21,777 molecules from QM9 are also in PC9 and 21,619 molecules from PC9 are also in QM9. The numbers are not identical since QM9 and PC9 contains a different amount of duplicate truncated InChi strings, so a structure from one dataset can appear multiple times in the other dataset.

In [13] it was reported that 18,357 structures from PC9 also belong to QM9, based on comparing InChi strings computed with the Open Babel software. We were not able to reproduce this number using any combination of InChi layers, so we instead used the method and result described above in this section.

B Additional results

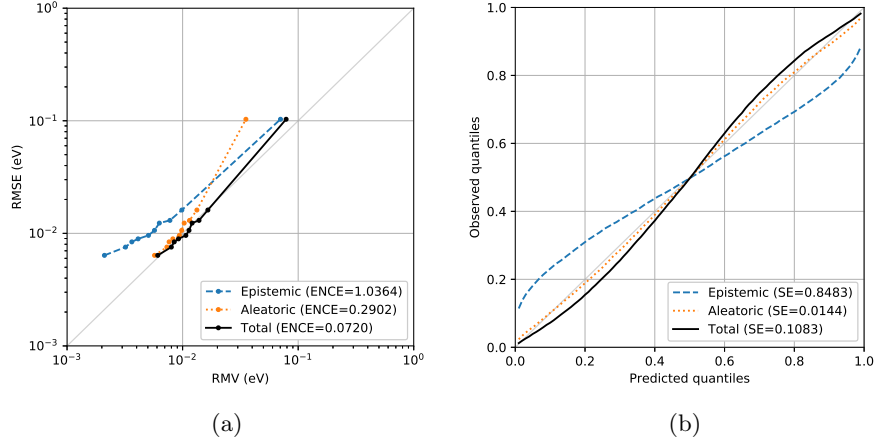


Figure B1: Evaluation of uncertainty on the QM9 test set when predicting E . Reliability diagram (a) and calibration plot (b).

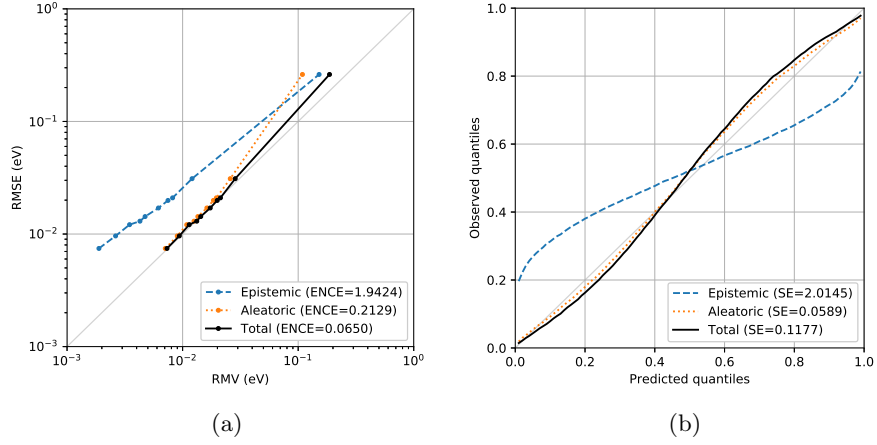


Figure B2: Evaluation of uncertainty on the PC9 test set when predicting E . Reliability diagram (a) and calibration plot (b).

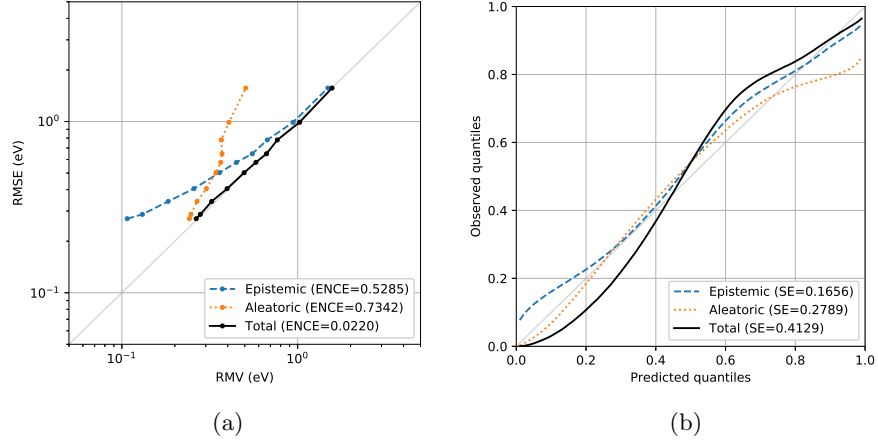


Figure B3: Evaluation of uncertainty when training on QM9 and testing on PC9. Reliability diagram (a) and calibration plot (b).

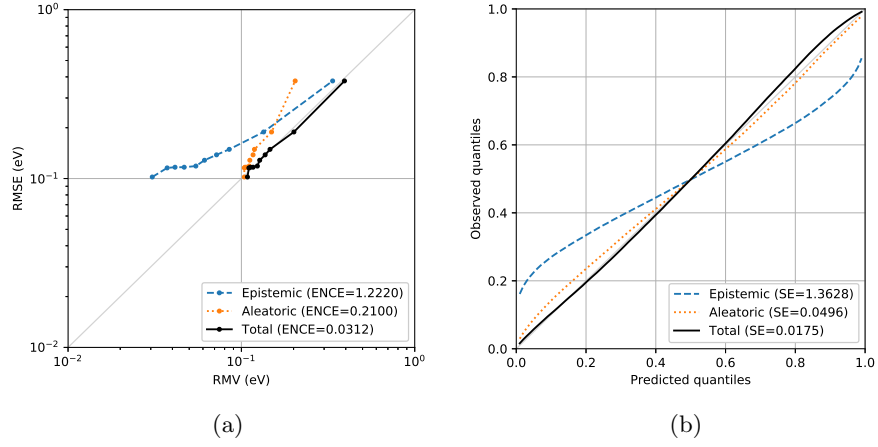


Figure B4: Evaluation of uncertainty when training on PC9 and testing on QM9. Reliability diagram (a) and calibration plot (b).